Neoplasia 63 (2025) 101152

Contents lists available at ScienceDirect

Neoplasia

journal homepage: www.elsevier.com/locate/neo

Original Research

Targeting BARD1 suppresses a Myc-dependent transcriptional program and tumor growth in pancreatic ductal adenocarcinoma

Sohum Patel [a], Eleanor Jenkins [a], Rutuj P Kusurkar [a], Sherry Lee [b], Wei Jiang [b], Avinoam Nevler [a], Matthew McCoy [c], Michael J Pishvaian [d], Rosalie C Sears [e], Jonathan R Brody [f], Charles J Yeo [a], Aditi Jain [a,1,*]

[a] Department of Surgery, Jefferson Pancreas, Biliary and Related Cancer Center, Thomas Jefferson University, Philadelphia, PA, USA
[b] Department of Pathology and Genomic Medicine, Thomas Jefferson University, Philadelphia, PA, USA
[c] Innovation Center for Biomedical Informatics & Lombardi Comprehensive Cancer Center, Washington, DC, USA
[d] Department of Oncology, The Johns Hopkins University School of Medicine, Baltimore, MD, USA
[e] Department of Molecular and Medical Genetics, and Brenden-Colson Center for Pancreatic Care Knight Cancer Institute, Oregon Health & Science University, Portland, OR, USA
[f] Department of Surgery, and Brenden-Colson Center for Pancreatic Care Knight Cancer Institute, Oregon Health & Science University, Portland, OR, USA

ARTICLE INFO

Keywords:
Pancreatic ductal adenocarcinoma
BARD1
PARP inhibitor
DNA damage
c-Myc

ABSTRACT

Pancreatic ductal adenocarcinoma (PDAC) remains one of the deadliest cancers demanding better and more effective therapies. BARD1 or BRCA1-Associated -Ring Domain-1 plays a pivotal role in homologous recombination repair (HRR). However, its function and the underlying molecular mechanisms in PDAC are still not fully elucidated. Here, we demonstrate that BARD1 is overexpressed in PDAC and its genetic inhibition suppresses c-Myc and disrupts c-Myc dependent transcriptional program. Mechanistically, BARD1 stabilizes c-Myc through ubiquitin–proteasome system by regulating FBXW7. Importantly, targeting BARD1 using either siRNAs or CRISPR/Cas9 deletion blocks PDAC growth *in vitro* and *in vivo*, without any signs of toxicity to mice. Using a focused drug library of 477 DNA damage response compounds, we also found that BARD1 inhibition enhances therapeutic efficacy of several clinically relevant agents (fold changes ≥4), including PARPi, in HRR proficient PDAC cells. These data uncover BARD1 as an attractive therapeutic target for HRR proficient PDAC.

Introduction

Pancreatic ductal adenocarcinoma (PDAC) is the most common malignant neoplasm of the pancreas, and it is anticipated to become the second highest cause of cancer-related mortality in the U.S by 2030 [1,2]. The 5-year overall survival rate for PDAC has doubled in the last decade, but still remains at a dismal 13 % [3]. The high mortality rate and poor outcomes of PDAC can be attributed to both late diagnosis and the presence of a harsh tumor microenvironment which makes treatment considerably more complex [4]. The current standard treatment regimens for PDAC revolve around surgical resection of the pancreas and systemic therapies with either FOLFIRINOX (5-fluorouracil, leucovorin, irinotecan, and oxaliplatin) or gemcitabine- nanoparticle albumin–bound (nab-) paclitaxel [2,5,6].

Although the cornerstone of systemic therapy for advanced or metastatic PDAC remains cytotoxic chemotherapy, recently, non-cytotoxic maintenance therapy with Poly- (ADP) -ribose- polymerase inhibitors (PARPi) have been actively explored. These drugs are a class of DNA repair inhibitors, that prevent the process of PARP1 enzyme mediated DNA repair at sites of DNA damage, causing PARP trapping and selective cell death in tumors where the homologous recombination repair (HRR) system is deficient [7,8]. Olaparib was the first approved PARPi by the FDA in 2019 for patients with metastatic PDAC harboring germline mutations in *BRCA1/2* genes [5,9,10]. Since then, many other PARPis are being evaluated either as single agent or in combination strategies for PDAC [5,11,12]. Our group also found the combination of veliparib (PARPi) and FOLFOX was safe for patients with metastatic PDAC in a Phase I/II clinical trial and showed promising activity in

* Corresponding author at: Department of Surgery, Jefferson Pancreas, Biliary and Related Cancer Center, Thomas Jefferson University, 1015 Walnut Street, Curtis Building, Room 618, Philadelphia, PA 19107 USA.
E-mail address: aditi.jain@jefferson.edu (A. Jain).
[1] Lead contact

https://doi.org/10.1016/j.neo.2025.101152
Received 13 January 2025; Received in revised form 6 March 2025; Accepted 6 March 2025

platinum-sensitive HRR deficient tumors [12]. Since, only a small proportion of PDAC patients have HRR deficiencies: for example, *BRCA* mutations are only found in about 5-10 % of PDAC cases, the utility of PARPis remains limited in the clinic [11,13]. Therefore, strategies to refine and expand this current narrow therapeutic scope are crucial.

BARD1 or BRCA1- Associated- Ring- Domain- 1 is a DNA repair protein, which forms an obligate heterodimer with BRCA1 via its N-terminus RING finger domain, facilitating the process of HR repair [14]. Studies have shown that the heterodimer not only aids in strand exchange after the loading of RAD51 on single stranded DNA in the process of HR repair, but it is also involved in the process of DNA end resection [15–17]. BARD1 also acts independent of BRCA1 and is necessary for cell survival and genomic stability [18,19]. Both BRCA1 dependent and independent functions of full-length BARD1 (FL-BARD1) suggest a tumor suppressor role of BARD1. However, many cancer predisposing mutations in *BARD1* (Q564H, V695L and S761N) compromise this tumor suppressor activity [20–23]. In PDAC patients, some incidences (0.1-0.8 %) of pathogenic variants in *BARD1* have also been observed [22,24–26]. Some studies have also found upregulation of BARD1 isoform expression in breast, ovarian, melanoma and hepatocellular cancers [20,27,28]. These isoforms are associated with disease progression, uncontrolled growth and proliferation of tumors, as well as invasion [29, 30]. Previously, we published that PDAC cells upregulate BARD1 in response to DNA damaging agents (PARPi and platinum) via an RNA binding post-transcriptional mechanism (HuR/*ELAVL-1*) and, inhibition of BARD1 enhances cell sensitivity to these two agents in HRR proficient PDAC, thus positing BARD1 as a therapeutic target to enhance efficacy of DNA damage response agents in HRR proficient PDAC [31]. While BARD1 has been explored by others as a therapeutic target in cancers of the colon, breast, and neuroblastoma, its functional and mechanistic role in PDAC is poorly understood [14,20,26,32].

Herein in this study, we characterized BARD1 as a therapeutic target in homologous recombination repair proficient PDAC and uncovered a crucial role of BARD1 in mediating stability of the oncoprotein, c-Myc. BARD1 inhibition abrogates PDAC cell and tumor growth and enhances efficacy of several DNA damage response agents. Our findings highlight and add to the rationale for potential anticancer strategies aimed at BARD1 for the treatment of PDAC patients, including those that harbor HRR -proficient tumors which comprise >90 % PDAC patient population.

Materials and methods

Cell culture

Pancreatic adenocarcinoma (PDAC) MiaPaCa-2, Panc-1, BXPC-3, HPAF and normal HPNE cell lines were obtained from American Type Culture Collection (Manassas, VA) and maintained in culture according to the manufacturer's instructions. All cell lines were cultured in DMEM with 10 % FBS at 5 % CO_2 and 37°C. CRISPR BARD1 Knockout MiaPaCa-2 pooled cell lines were purchased from Synthego (Menlo Park, CA). A single guide RNA (CUUCUCCAGGCGGUCGAGCG) against Exon 1 of Human BARD1 (Transcript ID: ENST00000260947.9) was used to generate knockout pools (Synthego Corp, Redwood City, CA), followed by single-cell FACS sorting and validation by Sanger sequencing, TOPO TA cloning and western blot analysis. All cell lines were STR authenticated and were tested for Mycoplasma monthly, using PCR based mycoplasma detection kit (#MP0035 Sigma Aldrich, St. Louis, MO). Cells were passaged at least twice after thawing and before experimental use.

Drugs and DNA damage compound library

PARP inhibitors were obtained from MedChem Express (Monmouth Junction, NJ). Cycloheximide and MG-132 were obtained from Sigma Aldrich. Stock solutions were diluted prior to use at indicated concentrations. DNA damage response drug library (96 well format) was purchased from Selleckchem (Houston, TX) and utilized as per manufacturer's instructions.

Drug screening

A library of DNA damage response agents (Table S1) was screened at a concentration of 10 μM (Selleckchem). Compounds were diluted and stored in FBS free culture media prior to treatment of 96-well plates. Scramble siRNA (SCR) or BARD1 siRNA (siB#1 and siB#2) transfected MiaPaCa-2 cells were plated on 96-well plates at a density of 800 cells per well. After 24 h, cells were treated in duplicate with drugs at the concentration of 10 μM in 0.01 % DMSO. DMSO-treated cells were used as controls. Cells were grown in 5 % CO_2 and 37°C for 5 days and cell survival was measured using Pico Green assay [31]. Data was normalized with values obtained from DMSO-treated control cells and plotted on scatter plot. Compounds that showed >50 % inhibition for siB and < 50 % inhibition for SCR control were selected and further studied.

siRNA transfections

All siRNA transfections were carried using RNAiMAX (Thermo Fisher Scientific, Waltham, MA) for 48 h according to the manufacturer's protocol. The following BARD1 siRNA was purchased from Thermo Fisher Scientific: siB#1:s1887 (5′-CGCUAUUGCUGCUACCAGATT-3′), and ON-TARGETplus Human BARD1 smartpool siRNA (siB#2: L-003873-00-0005) was purchased from Horizon Discovery Ltd. (Cambridge, UK) and used as previously described [33]. Non-targeting siRNA (siSCR) (D-001810-01-20) was purchased from Horizon Discovery Ltd.

RT-qPCR and mRNA expression analysis

Total RNA was extracted using the RNeasy mini kit (Qiagen Inc., Germantown, MD). 2 μg total RNA was used to make complementary DNA (cDNA) using the High Capacity cDNA Reverse Transcriptase kit (Life Technologies Corp). Quantitative PCR (RT-qPCR) was performed as previously described [31,34,35]. Relative quantification was performed using the 2-ΔΔCt method. A list of primers used in the study is included in the Table S2.

Genomic DNA extraction and sequencing

Genomic DNA of human PDAC cell lines was extracted by using the DNeasy Blood & Tissue Kit (Qiagen Inc., Germantown, MD) following the manufacturer's protocol. PCR was performed using a DNA thermal cycler and a set of primers. PCR products were analyzed by agarose gel electrophoresis and Sanger sequenced using specific primers.

Cell survival analysis

Cell survival and IC50 values were analyzed by Pico Green assay as previously described [31,35]. Percentage of relative cell survival was calculated and plotted using Graph Pad Prism 9.2.0 software.

GR50 analysis

Growth rate inhibition (GR) and GR_{50} values were analyzed by Pico Green assay and calculated using a published and validated GR calculator (http://www.grcalculator.org/grtutorial/Home.html) [36].

Colony formation assay

Colony formation assays were conducted in 6-well plates. 500-2000 cells were plated in each well and colonies were allowed to form for 14 days [31,35,37]. Colonies were first fixed in 100 % methanol and then stained with freshly prepared Coomassie blue solution (0.05 % Coomassie blue in 80 % methanol and 20 % water). Colonies were counted

using ImageJ software and graphed using Graph Pad Prism 9.2.0 software.

Matrigel boyden chamber invasion assays

The assay was performed as per the manufacturer's instructions. Briefly, cells were transfected with siRNAs, and serum-starved overnight. 5×10^4 cells in serum free media were placed in the top well of Matrigel invasion chambers (BD Biosciences, Chicago, IL), with 20 % FBS media (chemoattractant) in the lower chamber. Cells were allowed to invade/migrate through the membrane for 24 h at 37 °C. After 24 h, cells on the upper surface of the membrane were removed with cotton swabs, membranes were cut and cells on the undersurface of the membranes were fixed in 100 % methanol, stained with crystal violet and all cells were counted [33].

Immunoblot analysis

Cells were lysed in ice cold RIPA buffer (Santa Cruz Biotechnology Inc., Dallas, TX) supplemented with fresh protease inhibitor cocktail, PMSF and phosphatase inhibitor sodium orthovanadate. Protein samples were made in 4X Laemmli buffer and fractionated on SDS-PAGE gels (Bio-Rad, Hercules, CA). Samples were transferred on PVDF membranes and probed with primary and secondary antibodies, before scanning and quantitation using Odyssey Infrared Imaging System (LI-COR Biosciences, Lincoln, NE) as previously described [31,34,35]. All primary and secondary antibodies were obtained commercially. Thermo Fisher Scientific: α-Tubulin; Cell Signaling Technology (Danvers, MA): c-Myc; Abcam (Boston, MA): BARD1 (ab226854).

Immunohistochemistry (IHC)

Tissue microarrays (TMAs) were purchased from TissueArray.Com LLC (PA483e and PA242e) and stained with BARD1 antibody. Briefly, antigen retrieval was performed on the Roche Ventana Discovery ULTRA staining platform using Discovery CCI (Roche cat#950-500) for a total application time of 64 min. The primary antibody BARD1 was diluted to 1:200 and incubated at 36 °C for 44 min. Secondary immunostaining used a horseradish peroxidase (HRP) multimer cocktail (Roche cat#760-500) and immune complexes were visualized using the UltraView universal DAB (diaminobenzidine tetrahydrochloride) detection kit (Roche cat#760-500). Slides were then washed with a Tris based reaction buffer (Roche cat#950-300) and counter-stained with Hematoxylin II (Roche cat #790-2208) for 8 min. Slides were scanned on an AperioScope (20X objective, 20X zoom; Vista, CA). Pathologists scored TMAs blindly on a microscope. All immunolabeled samples were given a total IHC score by a surgical pathologist, equivalent to the labeling intensity score (0, negative staining; 1, moderate staining; or 2, strong staining) multiplied by a score reflecting the percentage of labeled cells (0-10 %=0, 10-50 %=1, >50 %−80 %=2).

RNA-sequencing

Total RNA was isolated from siRNA (siB and SCR) transfected Panc-1 and MiaPaCa-2 cells using RNeasy minikit (Qiagen) and sequenced (Novogene Co., Ltd., Sacramento, CA). Briefly, paired-end, 150-cycle eukaryotic RNA-Seq was performed using the Illumina Novaseq 6000 platform. Reference genome and gene model annotation files were downloaded from genome website browsers (NCBI/UCSC/Ensembl) directly. Index of the reference genome was built using Hisat2 v2.0.5 and paired-end clean 1 reads were aligned to the reference genome using Hisat2 v2.0.5. For DESeq2 with three to four biological replicates), differential expression analysis of two conditions/groups was performed using the DESeq2Rpackage (1.20.0). DESeq2 provide statistical routines for determining differential expression in digital gene expression data using a model based on the negative binomial distribution. The resulting P-values were adjusted using Benjamini and Hochberg's approach for controlling the false discovery rate. Genes with an adjusted P-value $\leq$0.05 found by DESeq2 were assigned as differentially expressed. Volcano plots were generated with Rstudio. Heat map was plotted using the values of the gene expression level (FPKM) normalized by the z-score method, from DESeq2 analysis.

GSEA

Gene Set Enrichment analysis (GSEA, version 4.0, Broad Institute, Cambridge, MA, USA) was performed on DEGs obtained from the RNA seq data of siBARD1 (siB) versus siSCR (SCR) (GEO Accession # GSE277278 and # GSE277280). Gene sets used were obtained from the Molecular Signatures Database (MSigDB, v 6.0; https://www.gsea-msigdb.org/gsea/index.jsp). Cancer hallmarks (H), KEGG signatures and Schuhmacher genesets were evaluated. We selected 1000 permutations and a false discovery rate (FDR $\leq$ 0.25); all other features were set to default settings.

Murine xenograft study

Athymic Nude-Foxn1nu male and female mice (Envigo RMS, Inc.) were subcutaneously injected with Mia CRISPR BARD1 and WT cells (5×10^6 cells/flank) in a 1:1 mixture of cold phosphate buffered saline (PBS): cold Matrigel (#356234 Corning). Mice body weight and tumor volumes were recorded three times per week. An event was recorded when tumor reached a volume (volume = (length x width^2)/2) of 100 mm^3 and plotted as Kaplan Meier curve for % mice with 100 mm3 palpable tumor as a function of time (days post injection). Mice were sacrificed if a reduction in body weight greater than 10 % was recorded or when the tumor volumes reached 1000 mm^3. Tumor growth in BARD1 (-/-) and BARD1 (±) study was followed until day 105 and day 70 respectively. Event free survival Kaplan-Meier curves were calculated using the log-rank Mantel-Cox. All mouse protocols were approved by the Thomas Jefferson University Institutional Animal Care and Use Committee.

Statistical analyses

Two sample t-test or one-way ANOVA were performed using GraphPad Prism software 9.2.0 (San Diego, CA). Results are expressed as mean ± SEM (standard error of mean) of at least three independent experiments, if not otherwise indicated.

Results

BARD1 is over-expressed in PDAC

BARD1 is overexpressed in PDAC tissues compared to normal pancreas ductal cells. Immunohistochemical staining was performed on commercially available PDAC tissue microarrays (TMA) which were also comprised of normal tissues, using a BARD1 specific antibody. The analysis revealed an increase in the intensity and percent staining of BARD1 in PDAC tissues compared to normal pancreatic ductal tissue, confirming the overexpression of BARD1 in PDAC at the protein level (Fig. 1a). Representative images of the TMA and different BARD1 staining intensities in PDAC versus normal ducts are shown in Figure S1.

We also performed RT-qPCR and protein analyses of different PDAC cell lines in culture and found that both BARD1 mRNA expression as well as protein expression were markedly increased across multiple PDAC cell lines including MiaPaCa-2, Panc-1, BXPC3, and HPAF compared to normal pancreatic cells represented by HPNE cells (Fig. 1b and c). Interestingly, BARD1 was overexpressed in BXPC-3, which is uniquely a KRAS wild-type, suggesting that BARD1 overexpression may occur independently of KRAS mutations, expanding the potential scope of BARD1 as a therapeutic target beyond KRAS-driven pathways.

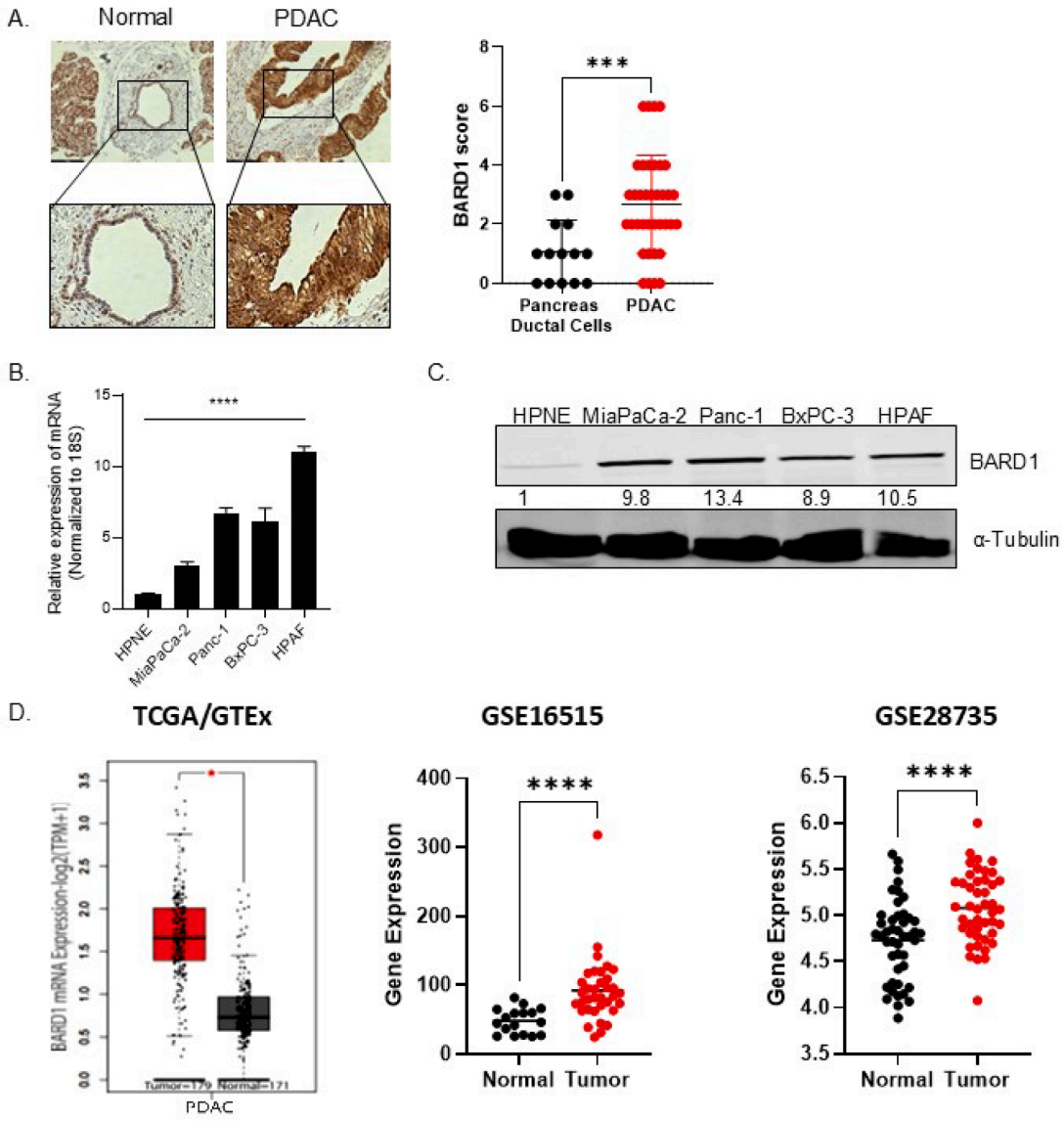

Fig. 1. BARD1 is overexpressed in PDAC. A) Immunohistochemistry staining of PDAC Tissue Microarrays with BARD1 antibody (left panel). The inset indicates BARD1 expression in the ductal cells. A representative graph of BARD1 IHC score is shown (right panel). *$p < 0.05$. B) mRNA expression and C) protein expression of BARD1 in PDAC cell lines compared to normal epithelial cell line, HPNE. Protein expression was normalized to α-tubulin and mRNA expression was normalized to 18s. ****$p < 0.0001$. D) BARD1 gene expression levels in PDAC and normal tissue from GEPIA using TCGA/GTEx data (left panel). |Log2FC| Cutoff: 0.5, p-value Cutoff: 0.01; GEO dataset GSE16515 (middle panel); GEO dataset GSE28735 (right panel) ****$p < 0.05$.

Moreover, analysis of the publically available patient data from TCGA/GTEx database and GEO datasets, which combine RNA expression from PDAC patients and normal, also confirm BARD1 is overexpressed in PDAC tissues versus normal tissues (*$p < 0.05$, Fig. 1d).

Targeting BARD1 disrupts the c-MYC-dependent transcriptional program

To explore the possible mechanism(s) by which BARD1 promotes PDAC malignancy and understand the functional role of BARD1 in pancreatic cancer, we transiently knocked down BARD1 using siRNA and performed RNA sequencing analysis on the RNA extracted from transfected PDAC cells (siB#1 or SCR siRNAs). A profile of differentially expressed gene (DEG) was obtained from the RNA sequencing analysis. Principal component analysis (PCA) revealed the DEG profiles of the two groups (siB#1 versus SCR) of cells and a volcano plot showing the number of upregulated and downregulated transcripts (padj< 0.05; log2FoldChange > 1 and <-0.1) (Fig. 2a and 2b). We also plotted a hierarchical clustering map (heatmap) of all the differentially expressed transcripts (Fig. 2c) and highlighted the downregulated and upregulated differentially expressed genes in siBARD1 (siB#1) vs SCR groups in all replicates ($n = 4$) based on Z-score of FPKM values. By performing Gene Set Enrichment Analysis (GSEA) across all Hallmark gene sets in the Molecular Signature Database (MSigDB) revealed the two MYC target gene sets as the most strongly downregulated gene sets. We also found negative enrichment of other gene sets related to MYC signaling (mTOR signaling, DNA repair, E2F targets, and EMT (Fig. 2d, e and Fig. S2). Negative enrichment of DNA repair/homologous recombination repair geneset is consistent with the established role of BARD1 as a DNA repair protein, validating our RNA seq results (Fig. S2). Based on the RNA seq results and to further verify the consistency and reproducibility of these results, we chose top DEG from the Hallmark_Myc_targets and analyzed the expression of several c-Myc target genes using independent RT-qPCR analysis and found these genes were also downregulated by the knockdown of BARD1 using a second siRNA (siB#2) in both Panc-1 and MiaPaCa-2 cells (Fig. 2f). These genes are involved in cell cycle, proliferation and ribosome biogenesis and are known to be positively

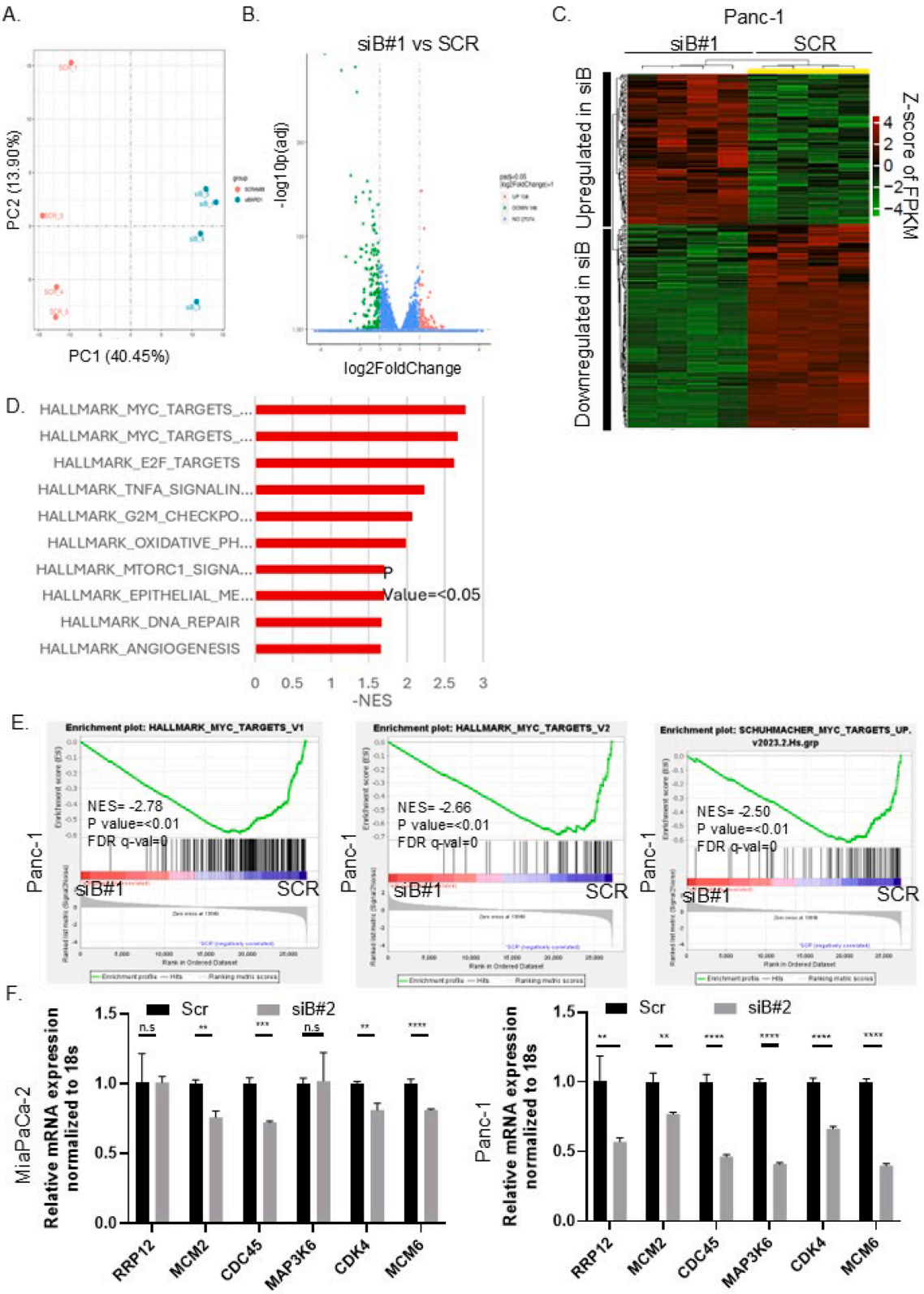

Fig. 2. RNA-seq analysis of Panc-1 PDAC cells treated with either SCR or BARD1 siRNA. A) Principal component analysis of all samples. B) Volcano plot showing gene-expression changes between SCR control and BARD1 siRNA (siB#1) cells. Downregulated transcripts, 186; upregulated transcripts, 138 (padj< 0.05; log2FoldChange > 1 and <−1). The x axis represents the fold change in gene expression and the y axis, the -log10 (adjusted p value). C) Hierarchical clustering map (heatmap) for differential expression genes in all samples ($n = 4$) based on Z-score (FPKM). Upregulated and downregulated genes in siB condition are marked. D) List of top 10 Hallmark genesets affected by targeting BARD1 in Panc-1 cells. $P < 0.05$. E) Gene Set Enrichment Analysis of siBARD1 (siB#1) vs. siSCR (SCR) ($n = 4$) samples in Panc-1 cells, showing negative enrichment of the Hallmark_MYC_targets and Schuhmacher_MYC_targets genesets. P Value, negative enrichment score (NES) and FDR q-value are mentioned. E) RT-qPCR analyses of selected genes from the MYC targets in MiaPaCa-2 and Panc-1 cell lines transfected with siB#2 and SCR. 6 common genes out of the top significant genes in the Hallmark_myc_v1 dataset ($n = 35$) were chosen ****$p < 0.001$.

regulated by MYC [38–41].

BARD1 enhances c-Myc protein stability

c-Myc, a protein which affects cellular proliferation and survival pathways, is frequently dysregulated in PDAC [42–46]. Since, c-Myc genesets were significantly enriched from our RNA seq data, we focused on analyzing the effects of targeting BARD1 on c-Myc expression. Our results show that depletion of BARD1 either transiently or through CRISPR-Cas9, significantly reduced the protein expression of c-Myc in PDAC cells (Fig. 3a). Surprisingly, no significant difference was observed in the mRNA levels of *c-Myc* when BARD1 was knocked down. Also, gene expression data from The Cancer Genome Atlas (TCGA) indicated a lack of correlation (Spearmen $r = 0.07$, $p = 0.321$) between the mRNA levels of BARD1 and c-Myc (Fig. 3b), while protein expression of c-Myc and BARD1 is positively correlated (Spearman $r = 0.87$, $p = 0.0001$) in the CCLE database (Fig. 3b). These results indicate that BARD1 might affect c-Myc via a protein stability or degradation mechanism. Therefore, we treated PDAC cell lines with the de novo protein synthesis inhibitor, cycloheximide (CHX), at several specific time points and as expected, treatment with CHX resulted in a faster degradation of c-Myc in the BARD1 knockdown cells, further supporting the notion that BARD1 stabilizes c-Myc protein (Fig. 3c). One of the most prominent mechanisms for c-Myc degradation in cells is through the ubiquitin–proteasome pathway. We investigated the effects of proteasome inhibitor, MG-132, on c-Myc expression in BARD1-depleted PDAC cells. As expected, MG132 significantly reversed the downregulation of c-Myc in siBARD1 transfected Panc-1 and MiaPaCa-2 cells, suggesting that BARD1's regulation of c-Myc is related to the ubiquitin proteosome process (Fig. 3d). Increased degradation of c-Myc was associated with increased ubiquitin proteosomal degradation in the BARD1 siRNA conditions (Fig. 3e). To understand which E3 ubiquitin ligases might be involved in this process, we analyzed the effect of BARD1 inhibition on the transcription levels of several known E3 ligases of c-Myc that destabilizes it [47–51]. As shown in Fig.. 3f, FBXW7 levels were most consistently increased in both MiaPaCa-2 and Panc-1 cells transfected with BARD1 siRNAs (Fig. S3). These results suggested that the presence of BARD1 stabilizes c-Myc.

Genomic silencing of BARD1 suppresses growth and invasion of PDAC cells

Herein, we studied the effects of targeting BARD1 on PDAC cell proliferation and invasion *in vitro*. Inhibiting BARD1 through transient knockdown using two different siRNAs (siB#1 and siB#2) effectively decreased cell proliferation of PDAC cells across various cell lines, including MiaPaCa-2, Panc-1, and BXPC3, which are all homologous recombination repair proficient. We observed these effects in a long-term colony formation assay conducted over a 14-day period (Fig. 4a and Fig. S4a). In contrast, expressing BARD1 exogenously using an overexpression plasmid enhanced cell proliferation of PDAC cells (Fig. 4b and Fig. S4b). Furthermore, we confirmed these findings by conducting short-term proliferation assays using Pico Green assay over a period of 10 days. Notably, cells transfected with BARD1 siRNAs (siB#1 and siB#2) exhibited markedly slower growth compared to control/scrambled siRNA transfected cells (Fig. 4c and Fig. S4c), and overexpressing BARD1 exogenously enhanced cell growth of MiaPaCa-2 cells. (Fig. 4d). We also utilized transient siRNA knockdown methods (siB#1 and siB#2) in Matrigel Boyden Chamber invasion assays to understand the role of BARD1 in PDAC invasion. Briefly, siRNA transfected cells in serum-free medium were seeded on the top of transwell inserts, with serum-rich medium (20 % FBS) in the bottom chambers, and cells were allowed to invade for 24 h. Notably, we found a significant decrease in relative invasion when BARD1 was transiently knocked down in both MiaPaCa-2 ($p < 0.05$) and Panc-1 ($p < 0.001$) cells (Fig. 4e).

To confirm the effects of targeting BARD1 via transient siRNAs on PDAC growth and invasion, we generated and utilized BARD1 CRISPR PDAC cells (clone c10.2: BARD1 (-/-) and c16: BARD1 (±), Fig. 5a and Fig. S5a). These models were established via CRISPR-Cas9 gene editing in MiaPaCa-2 cells, and deletion/mutation was confirmed using western blot analysis and Sanger sequencing (Fig. 5a and 5b). Colony formation assays conducted over a span of 14 days revealed significantly decreased cell proliferation in both the BARD1(±) and BARD1(-/-) models compared to WT MiaPaCa-2 cells (Fig. 5c and Fig. S5b). These results were replicated using Pico Green assay and a similar inhibition in relative cell growth over time was observed in BARD1 (-/-) vs WT CRISPR models (Fig. 5d). BARD1 (-/-) cells also invaded less in Matrigel Boyden assay ($p < 0.001$), replicating results from the transient knockdown of BARD1 via siRNAs (Fig. 5c).

CRISPR-Cas9 deletion of BARD1 delays PDAC growth in vivo

Because our *in vitro* studies suggested a functional role for BARD1 in PDAC proliferation and growth, we investigated the contribution of BARD1 to PDAC growth *in vivo*. Female and male nude mice were subcutaneously injected with either BARD1 WT, BARD1 (±), or BARD1 (-/-) MiaPaCa-2 cells. Mouse were sacrificed when the tumor volumes reached/crossed 1000 mm^3. To assess the role BARD1 plays on tumor growth *in vivo*, we first measured the time (days) it took for the tumors to reach a measurable size (palpable tumor), which we defined as 100 mm^3. BARD1 WT tumors began forming around day 12 post injection (p.i), whereas BARD1 (-/-) tumors began forming around day 47 (Fig. 5e). Only 13 % of mice injected with BARD1(-/-) cells had a palpable tumor by day 52 of the study (half way through completion of the study), compared to WT, in which 100 % of the mice had tumors as early as day 23 (Fig. 5f). This indicates that targeting BARD1 substantially slows PDAC tumor growth *in vivo*. Additionally, mice with BARD1 (-/-) tumors were also observed to have an increase in survival ($p = 0.002$), as analyzed by the Kaplan Meier plot (Fig. 5g). However, no significant survival advantage was seen in mice with BARD1 (±) tumors (Fig. S5d). Individual tumor volumes are shown in the spaghetti plot (Fig. 5h and Fig. S5e). Mouse weights remained consistent with no significant differences observed in the experiment group as compared to the control group (Fig. 5i). Overall, these findings underscore BARD1 serves an oncogenic role, in promoting PDAC cell proliferation and growth.

Inhibition of BARD1 enhances therapeutic efficacy of DNA damage response agents

We investigated the therapeutic potential of BARD1 as a target in HRR proficient PDAC (MiaPaCa-2 and Panc-1), using two different BARD1 siRNA models (siB#1 and siB#2) and subjected the cells to DNA damage drug library for dose response studies using Pico Green assays (Fig. 6a). The cells were exposed to the DNA damage drug library composed of a diverse collection of 477 small molecules that are known to function through DNA damage response pathways (Table S1). We assessed the change in percent inhibition of survival in siBARD1 cells relative to SCR control cells. Any drug demonstrating >50 % inhibition in siBARD1 (siB#1 and siB#2) treatments and <50 % inhibition in SCR control treatments was flagged as potentially more effective upon BARD1 inhibition. Using the siB#1, 40 drugs exhibited greater than 50 % inhibition, while in the siB#2 experiment, 34 drugs showed greater than 50 % inhibition (Fig. 6b). Notably, 15 compounds commonly displayed >50 % inhibition in both experimental models (Fig. 6c and d). These compounds were highlighted as promising candidates for further investigation due to their consistent efficacy in reducing survival of BARD1 targeted cells.

Out of the 15 hit compounds, 5 (Olaparib, Rucaparib, Veliparib, AZD-2461 and Pamiparib) belong to the PARP inhibitor class of drug family [7,11,52,53]. Using our CRISPR-Cas9 BARD1KO cells we assessed cell survival *in vitro* following exposure to four of these PARP inhibitors, in separate Pico Green assays to validate the results from the

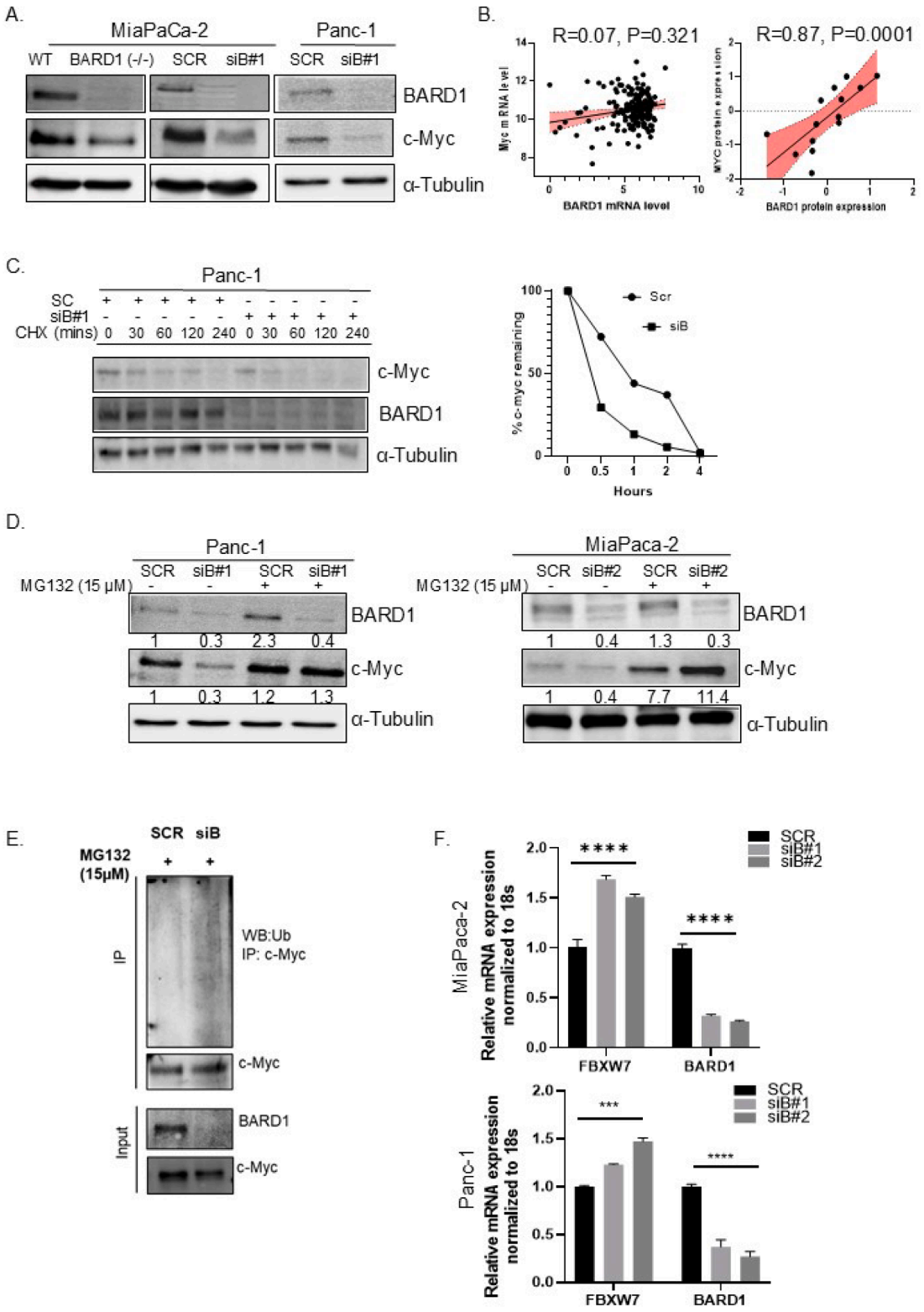

Fig. 3. BARD1 enhances c-Myc stability in PDAC. A) Western blot analysis showing endogenous c-Myc protein levels in BARD1 CRISPRKO PDAC cells and cells transfected with either BARD1 siRNA (siB#1) or SCR. B) Correlation plots of BARD1 and c-Myc mRNA (left) and protein (right) levels from TCGA and CCLE datasets. Spearman r and p values are mentioned. C) Effect of cycloheximide (CHX, 25 μg/ml) on c-Myc stability in BARD1 depleted Panc-1 cells. The protein expression of BARD1 and c-Myc was analyzed by western blotting. Graph represents % c-Myc remaining at each time point. D) Effect of MG-132 (15 μg/ml) on c-Myc expression in BARD1 depleted (siB) and SCR control Panc-1 and MiaPaCa-2 cells. The protein expression of BARD1 and c-Myc was analyzed by western blotting and normalized to α-Tubulin. Numbers represent relative expression to SCR. E) Immunoprecipitation (IP) was used for the detection of c-Myc degradation in MiaPaCa-2 cells transfected with BARD1 siRNA and SCR siRNA. After treating indicated cells with MG-132 (15 μM) for 6 h, extracts were subjected to IP with c-Myc antibody and the poly-ubiquitination of c-Myc was assessed by western blot using ubiquitin antibody. Corresponding input controls are also shown. F) RT-qPCR analyses of FBXW7 in MiaPaCa-2 and Panc-1 cell lines transfected with siB and SCR. $^{****}p < 0.001$, $n = 3$.

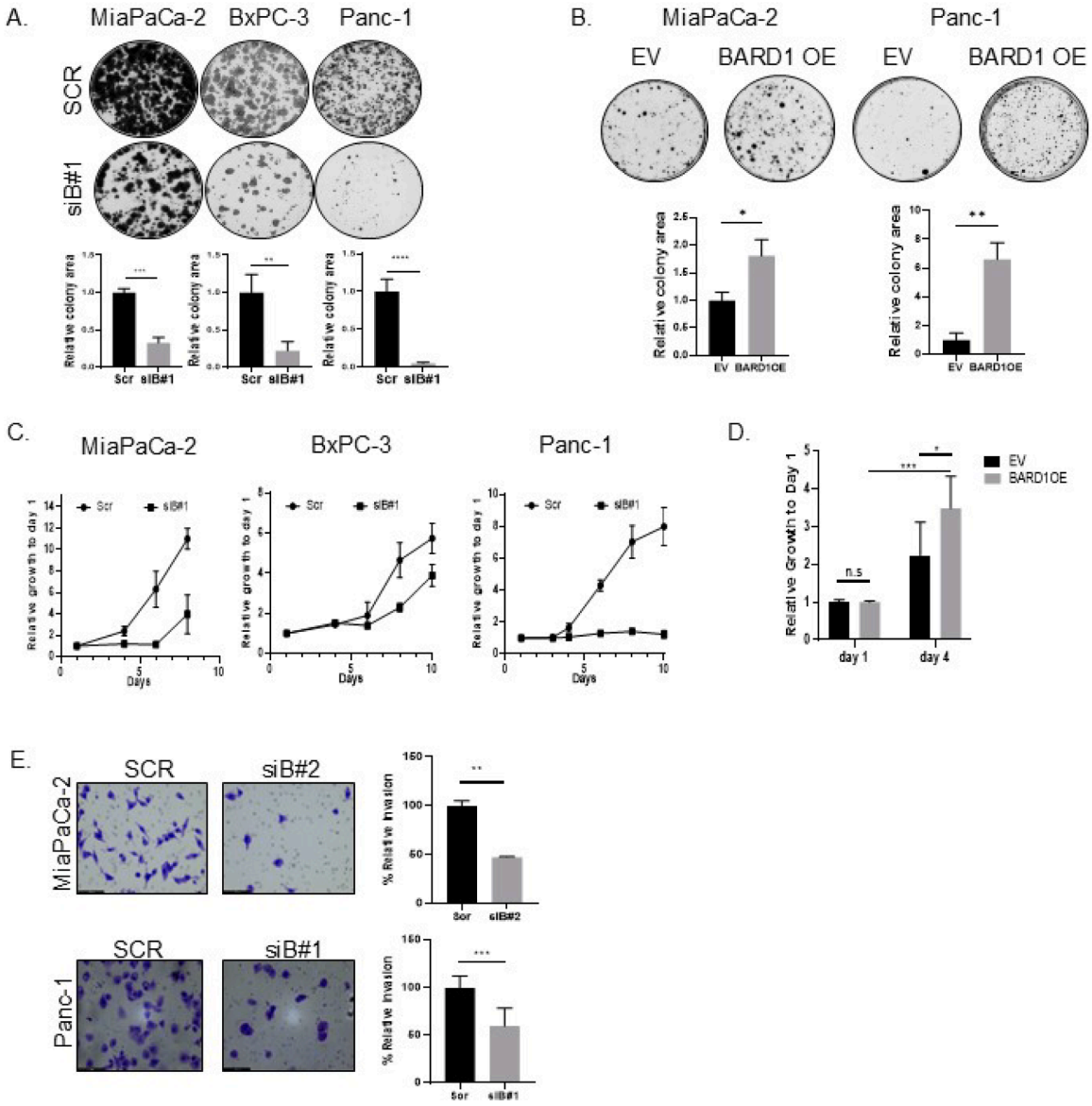

Fig. 4. BARD1 is required for PDAC proliferation and invasion. Colony formation assay of A) PDAC cell lines (MiaPaCa-2, Bxpc-3, Panc-1) transfected with either BARD1 siRNA (siB#1) or Scramble siRNA, and B) BARD1 overexpressed (BARD1OE) and empty vector (EV) MiaPaCa-2 and Panc-1 cells. Colonies were stained with crystal violet solution after 14 days. Representative pictures and graph of relative colony area from $n = 3$ are shown. Growth of PDAC cell lines transfected with C) either BARD1 siRNA (siB#1) or Scramble siRNA (SCR), and D) BARD1 overexpression plasmid or EV. Graphs represent growth relative to day 1 as analyzed by Pico Green assay. E) MiaPaCa-2 and Panc-1 cells transfected with BARD1 siRNA (siB) or Scramble siRNA (SCR) for 48 h, were utilized in Matrigel Boyden chamber invasion assays. Representative images are shown. Graphs are Mean ± SEM for three independent experiments; each experiment was normalized to Scrambled (SCR) control. n.s=not significant, $*p < 0.05$, $**p < 0.01$, $***p < 0.001$.

drug library. We found that knocking out BARD1 sensitized PDAC cells to Olaparib, Rucaparib, Veliparib, and AZD-2461 (fold changes ≥4), the latter is a novel PARP inhibitor currently in Phase 1 clinical trials (Fig. 6e). IC50 values are shown in the table accompanying the figure. Since BARD1 CRISPR KO cells grow slower compared to WT cells as shown in Fig. 5 above, we also plotted GR50 curves to account for growth rate using the above drugs and found similar results (Fig. S6a). The results from the drug library were also consistent across both the MiaPaCa-2 and Panc-1 cell lines transiently transfected with either BARD1 siRNA (siB#2) or SCR control in separate Pico Green cell survival assays (Fig. S6b). In fact, ectopic expression of BARD1 in PDAC cells reversed this phenotype and led to drug resistance (Fig. S6c), suggesting BARD1 is crucial for the therapeutic efficacy of PARP inhibitors in PDAC. Overall, these results reinforce the therapeutic potential of targeting BARD1 in PDAC.

Discussion

Many cytotoxic chemotherapies, targeted therapies, and immunotherapies that work for other cancers with similar poor prognoses as PDAC do not work for PDAC patients, and the overall 5-year survival rate for PDAC patients remains the lowest (SEER*Explorer, https://seer.cancer.gov). Consequently, developing novel strategies that will benefit patients with this aggressive disease is imperative. Here, we identified BARD1 as an exploitable therapeutic target for PDAC, which stabilizes the oncoprotein c-Myc, and identified several DNA damage response agents that show increased efficacy when BARD1 is targeted in HRR proficient PDAC.

DNA damage response (DDR) pathways are essential for maintaining genome integrity following various forms of DNA damage, including base modifications, single-strand or double-strand DNA breaks, or

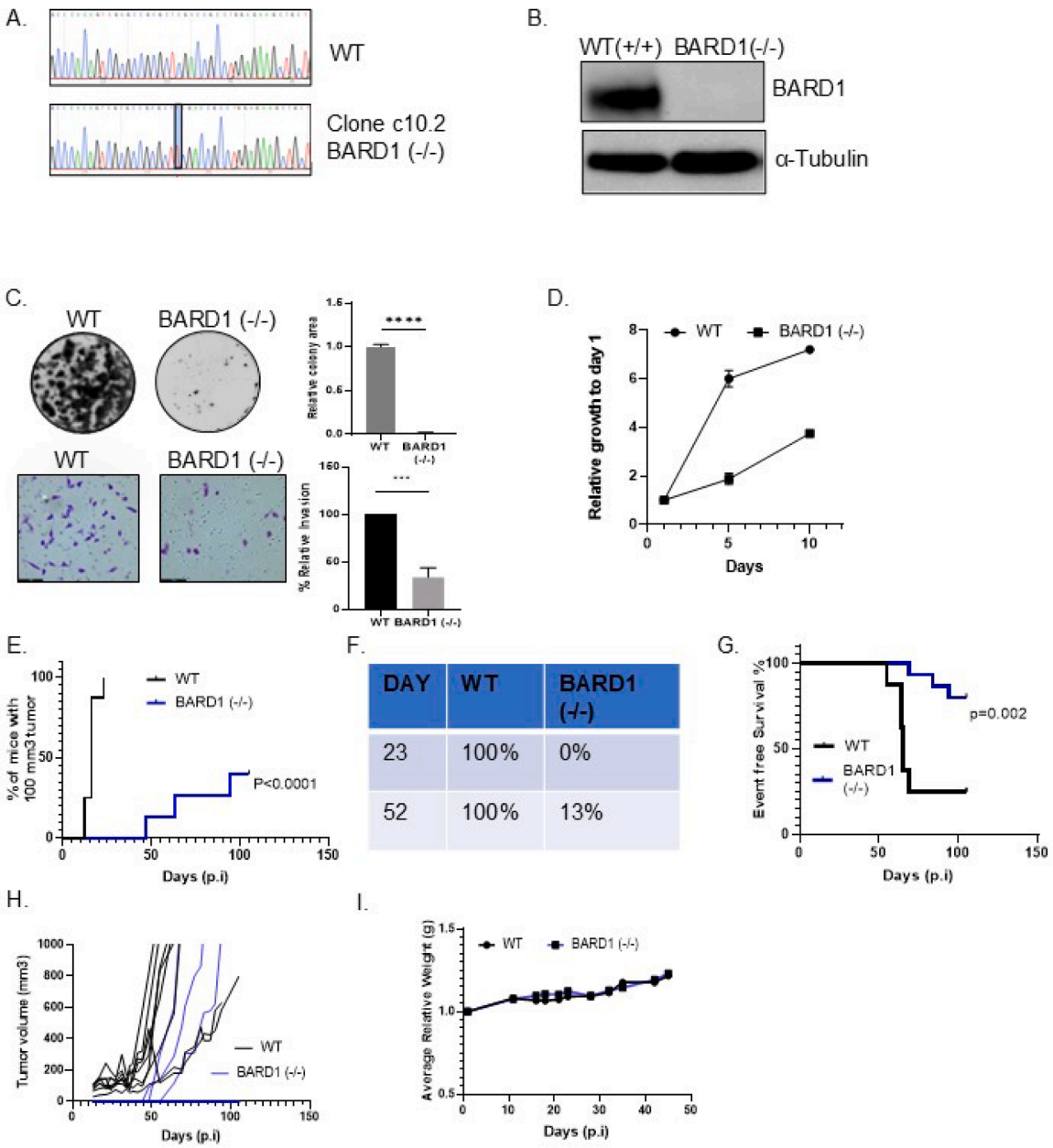

Fig. 5. CRISPR-Cas9 deletion of BARD1 slows PDAC growth in vitro and in vivo. A) Chromatograms from Sanger sequencing of wild type BARD1 WT (+/+) and homozygous mutant BARD1 (-/-) clones, generated by CRISPR-Cas9 transfection in MiaPaCa-2 cells. Highlighted in red is the specific mutations in the BARD1 (-/-) clone. B) Relative protein expression of BARD1 in CRISPR clones by western blot analysis. α-Tubulin was used as a loading control. C) Colony formation (top) and Matrigel Boyden invasion (bottom) assay with WT and BARD1 (-/-) MiaPaCa-2 cells. Representative images and graphs of relative colony area and relative invasion from $n = 3$ are shown.****$p < 0.0001$. D) Growth curves of WT and BARD1 (-/-) MiaPaCa-2 cells relative to day 1. E) Graph showing percentage of mice that developed palpable tumors of 100 mm3. F) Table showing percentage of mice with 100 mm3 tumors post injection. G) Kaplan Meier survival curve in a xenograft tumor model after injection of WT and BARD1 (-/-) CRISPR mutant cells into flanks of nude mice (n= 8 for WT, n = 15 for BARD1 (-/-)). H) Spaghetti plot of individual tumor volumes. I) Mouse weights plotted over time. Note: Mouse weights averages until day 45 are shown because of staggering survival events that decrease the number of mice in each experimental group.

intrastrand and interstrand DNA cross-links [54]. Among these pathways, the two principal mechanisms for repairing double-strand breaks are the homologous recombination repair (HRR) and error prone non-homologous end joining (NHEJ) [54]. Defects or mutations in DDR pathways, one of the hallmarks of cancer, are closely linked with the development of malignancies. For example, defects in HRR due to *BRCA1/2* mutations often lead to genomic instability and cancer progression [55,56]. In the case of PDAC, around 5-10 % of the patient population harbor defects in the *BRCA1/2* gene (germline or sporadic mutations), and therefore may benefit from a personalized treatment approach [10,11,57]. In 2019, the FDA approved the PARP inhibitor, Olaparib in the maintenance setting for metastatic PDAC patients with a germline *BRCA1/2* mutation, previously treated with a platinum-based chemotherapy [10]. This approval came after the success of the POLO trial which demonstrated a progression-free survival (PFS) benefit with Olaparib [10]. It not only set the stage for "precision" oncology for pancreatic cancer but also shifted the paradigm of PDAC management. Besides deficiency/inactivating mutations in the DDR pathways, the acquired or inherent adaptation of cancer cells to either resist treatment, survive in a harsh tumor micro-environment, and progress/metastasize is linked to upregulation of DDR proteins, and provide cancer-specific vulnerabilities that can be exploited therapeutically either in

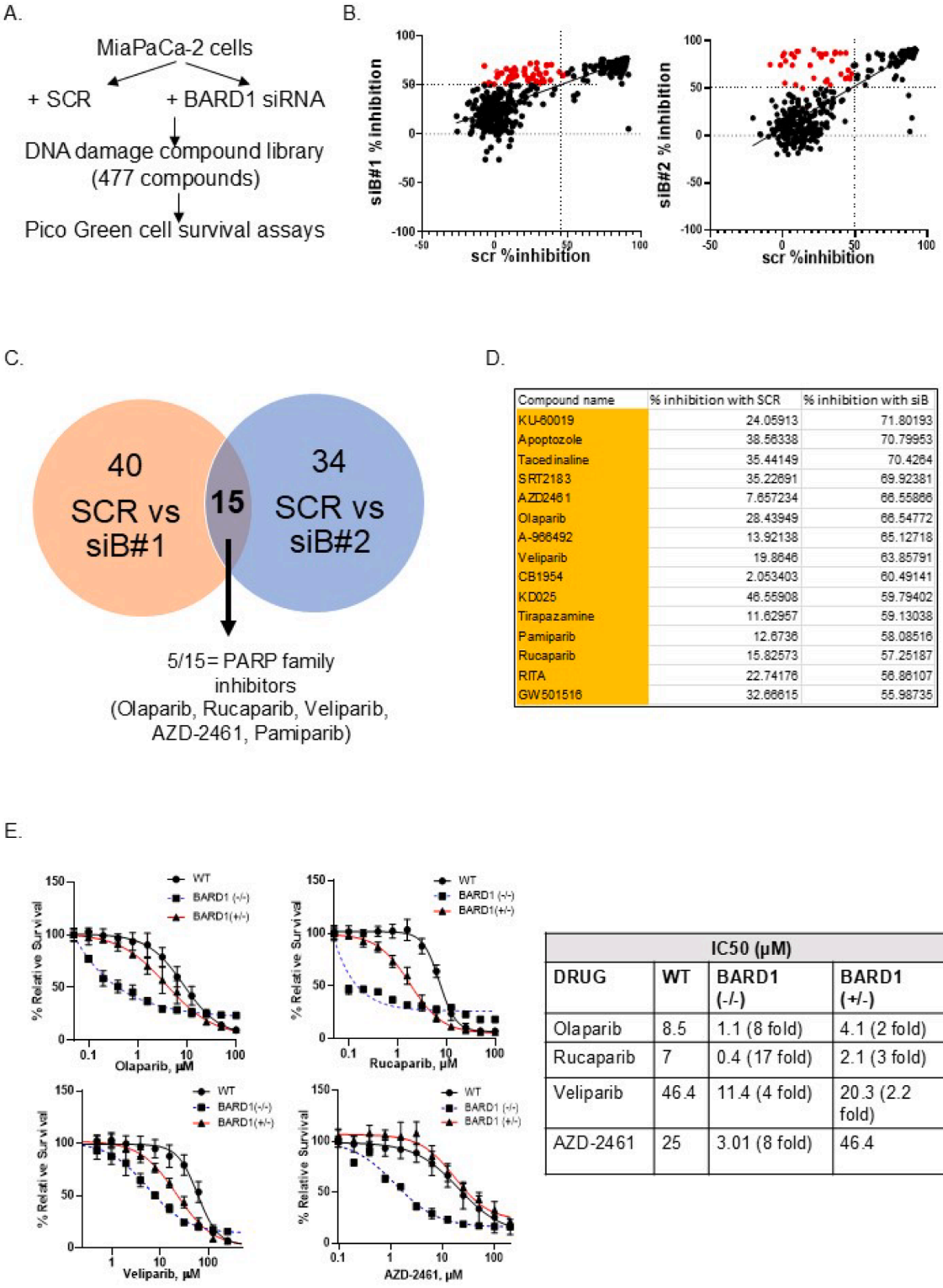

Compound name	% inhibition with SCR	% inhibition with siB
KU-60019	24.05913	71.80193
Apoptozole	38.56338	70.79953
Tacedinaline	35.44149	70.4264
SRT2183	35.22691	69.92381
AZD2461	7.657234	66.55866
Olaparib	28.43949	66.54772
A-966492	13.92138	65.12718
Veliparib	19.8646	63.85791
CB1954	2.053403	60.49141
KD025	46.55908	59.79402
Tirapazamine	11.62957	59.13038
Pamiparib	12.6736	58.08516
Rucaparib	15.82573	57.25187
RITA	22.74176	56.86107
GW501516	32.66615	55.98735

IC50 (μM)			
DRUG	WT	BARD1 (-/-)	BARD1 (+/-)
Olaparib	8.5	1.1 (8 fold)	4.1 (2 fold)
Rucaparib	7	0.4 (17 fold)	2.1 (3 fold)
Veliparib	46.4	11.4 (4 fold)	20.3 (2.2 fold)
AZD-2461	25	3.01 (8 fold)	46.4

Fig. 6. Targeting BARD1 enhances efficacy of various DNA damage response agents. A) Flow chart of drug screening experiment. B) Graphs showing percentage inhibition in survival of BARD1 siRNA (siB#1 and siB#2) and SCR control MiaPaCa-2 PDAC cells after exposure to different drugs from the drug library. Red dots depict compounds that show >50 % inhibition with siBARD1 and <50 % inhibition with Scramble (SCR) treatments. C) Venn diagram showing common agents in the two siRNA groups (siB#1 and siB#2). D) Table of common agents with % inhibition. E) Graphs showing % relative survival in WT, BARD1 (-/-) and BARD1 (±) CRISPR mutant cells after indicated drug treatments for 5 days, as analyzed by Pico Green assay. Table on the right shows IC50 (μM) and fold change values for each condition. All experiments were performed atleast $n = 3$.

combination strategies, or as ideal monotherapies [52,58–61]. Our prior research identified that BARD1 is upregulated at both mRNA and protein levels in cells exposed to either PARP inhibitors or platinum agents. This upregulation occurs through a post-transcriptional RNA binding mechanism, imparting a resistance mechanism to these DNA damage agents [31].

In this study, we explored the potential of BARD1 as a therapeutic target in PDAC. We demonstrated that BARD1 is widely upregulated in both PDAC tissues and pancreatic cancer cell lines as compared to normal cells (Fig. 1). We utilized genomic approaches to target BARD1 by either transiently silencing its expression using siRNAs or by creating and utilizing a CRISPR-Cas9 BARD1 KO cell model. Our findings demonstrate that inhibiting BARD1 either by siRNA or by CRISPR-Cas9 approaches results in slow proliferation of PDAC *in vitro* and *in vivo*, whereas exogenous overexpression of BARD1 in PDAC cells enhanced proliferation (Fig. 4 and 5). Intriguingly, BARD1 is classically known as a tumor suppressor, as it heterodimerizes with BRCA1 in the process of HRR, but our data support the notion that BARD1 has important oncogenic roles to play in PDAC and is pro-proliferative. Our data complements many published results in other cancer types that have suggested the tumorigenic potential of BARD1, perhaps via its spliced isoforms, but none have studied the effects of targeting BARD1 [21,24,25,28,29]. Our findings also suggest that a broader therapeutic potential for BARD1 exists in PDAC patients, beyond only mutant KRAS-driven PDAC subtypes as similar growth inhibitory results were obtained after targeting BARD1 in the BXPC-3 cell line, which lacks the common KRAS driver mutations found in the majority (>90 %) of PDAC [62].

We further studied tumor growth of BARD1 CRISPR KO cells *in vivo* in a nude murine model with subcutaneous xenograft tumors and found similar results from our *in vitro* studies. Tumor growth (palpable tumors) of BARD1 (-/-) cells in mice was delayed by over 4 weeks and only 13 % of mice bearing BARD1KO (-/-) tumors had developed tumors of 100 mm^3 (small palpable tumor) by day 52, by that time all WT (100 %) mice had developed tumors of or over 100 mm^3 (Fig. 5). For the BARD1 (±) group, 86 % of the mice had developed palpable tumors. BARD1KO (-/-) mice also survived significantly longer ($p = 0.002$) than either the mice with WT tumors or the mice bearing BARD1 (±) tumors, suggesting BARD1 plays a role in proliferation and growth of PDAC. Interestingly, in the harvested tumors of mice injected with BARD1 KO (-/-), we found no differences in the DNA sequence of cells that were injected initially at the start of the study and ones that were harvested (Fig. S5f), confirming that no other genetic alteration(s) occurred between the time of tumor engraftment until harvest, which could have led to the proliferation of BARD1 KO (-/-) cells. Since a subcutaneous model does not recapitulate the tumor microenvironment in its absolute sense, and contributing factors surrounding tumor in the tissue could influence the growth, we are aware of the clinical limitations of a xenograft model in this study. Hence, based on these results, we are developing a conditional knockout model which we will utilize in a more clinically relevant orthotopic mouse model in the future. Overall, these results implicate that targeting BARD1 may delay/slow tumor growth and will allow the extension of therapeutic window in which the drugs can be effectively administered to patients at lower doses for a longer duration, which is likely to have a positive impact on treatment outcomes for PDAC patients. Inhibition of BARD1 also led to inhibition of PDAC cell invasion and downregulation of markers involved in epithelial to mesenchymal transition (EMT), further substantiating that BARD1 supports PDAC malignancy.

To better understand the mechanisms behind BARD1's functional role in PDAC, we performed an RNA seq whole transcriptome analysis of BARD1 silenced cells as compared to SCR control (Fig. 2). Our data demonstrates that targeting BARD1 modulates several cancer related transcripts and pathways involved in DNA repair, proliferation, EMT, cell cycle of PDAC cells. This is the first study to show that BARD1 inhibition impacts c-Myc and several c-Myc target genes (Fig. 2 and 3), some of which are either associated with cell cycle progression (RRP12, CDK4) or DNA replication (MCMs, CDC45), and we speculate that BARD1's oncogenic/tumorigenic potential in PDAC is dependent on its interaction with the proto-oncogene c-Myc and its associated transcriptional activity [38–41,44,63]. c-Myc is a well-known oncogene and is a master transcription factor that regulates gene expression by binding to the promoter region of many cellular genes involved in cancer cell proliferation, metastasis, survival and metabolism [64,65]. It is a common dysregulated oncogene in PDAC, and it has been shown that Myc activity is a major determinant of metastatic burden and chemosensitivity in advanced PDAC [64–66]. Moreover, conditional inactivation of c-Myc is sufficient to induce disassembly of PDAC back to PanINs, causing death of tumor cells [67]. Although the exact mechanisms of c-Myc activation in PDAC remain largely unknown, it is mostly indirectly contributed by the upstream aberrant KRAS signaling, which is prevalent in greater than 90 % of PDAC [43,64,68]. Our study shows that BARD1 and c-Myc expression are positively correlated, since knocking down BARD1 decreased c-Myc protein expression. Our results also indicate that BARD1 stabilizes c-Myc protein via inhibition of its degradation via the ubiquitin proteosome pathway, a critical pathway by which c-Myc is degraded in cells [69]. We found that the expression of FBXW7, one of the E3 ligases that degrade c-Myc is regulated by BARD1. However, the exact molecular mechanism by which this occurs represents a new function for BARD1 and is part of ongoing research. Future studies are also intended to evaluate the role of c-Myc in facilitating transcription of BARD1 isoforms and BARD1 dependent PDAC tumorigenesis by utilizing GEMM models *in vivo*.

From a therapeutic perspective, since a direct chemical inhibitor for BARD1 is not yet available, we inhibited BARD1 genetically and conducted a drug response analysis using a DNA damage response drug library to investigate synthetic lethality with other agents beyond those previously studied by us, such as Olaparib and Oxaliplatin [31]. Given the limited overall efficacy of PARP inhibitors, especially in the maintenance setting, it is crucial to develop upfront combination strategies for PDAC patients, majority of which harbor HRR proficient tumors. Our current findings reinforce and expand on our previously published results and further substantiate that targeting BARD1 in HRR proficient PDAC (MiaPaCa-2 and Panc-1) uniquely sensitize them to several DNA damage response/ DNA repair inhibitors (Fig. 6). The future goals are to understand the *in vivo* effects of targeting BARD1 and these inhibitors together, and to design and develop therapeutic strategies to inhibit BARD1 expression and activity in PDAC and other cancer types.

Conclusions

In summary, the data presented here strongly supports that BARD1 is an exploitable therapeutic target for PDAC tumors that share molecular features with HRR proficient PDAC subtypes. BARD1's oncogenic roles as opposed to its tumor suppressor properties (BRCA1 dependent and independent) in PDAC malignancy have not been well characterized before. This study provides the first proof-of-principle evidence to suggest that BARD1 has distinct oncogenic roles to play in PDAC malignancy and that acute targeting of BARD1 should be pursued as an anticancer treatment strategy for PDAC even in HRR-proficient genetic backgrounds. The study also provides a new direction for several DNA damage response targeted strategies for PDAC.

Appendix. Supplemental information

Figures S1–S6 related to main figures 1-6.

Table S1 and S2. Excel file containing list of primers used and DNA damage response drug library index.

Funding

This work was supported by grants (to A.J.) from the Pancreatic Cancer Action Network-Career Development Award, 21-20-JAIN; NIH/NCI-RO3 (1R03CA283232-01); and the Saligman Research Funds from

the Department of Surgery, TJU. JRB was supported by grants from the NIH (R21 CA263996; RO1 CA212600, UO1 CA224012) and grants from the Brenden-Colson Center for Pancreatic Cate at OHSU, Hirshberg Foundation and the Sarah Parvin Foundation. The Core facilities of the Sidney Kimmel Cancer Center at Jefferson University were supported by a Cancer Center Support grant from the National Cancer Institute, 5P30CA056036-17.

Data availability

The RNA-seq datasets supporting this study are available in the NCBI Gene Expression Omnibus (GEO), under the accession numbers # GSE277278 and # GSE277280. All other data generated or analyzed during this study are included in this published article, and available upon reasonable request to the corresponding author.

CRediT authorship contribution statement

Sohum Patel: Writing – review & editing, Writing – original draft, Validation, Methodology, Investigation, Formal analysis, Data curation, Conceptualization. **Eleanor Jenkins:** Writing – review & editing, Writing – original draft, Validation, Methodology, Investigation, Formal analysis, Data curation. **Rutuj P Kusurkar:** Writing – review & editing, Validation, Methodology, Investigation, Formal analysis, Data curation. **Sherry Lee:** Writing – review & editing, Methodology, Investigation, Formal analysis, Data curation. **Wei Jiang:** Writing – review & editing, Resources, Methodology, Formal analysis, Data curation. **Avinoam Nevler:** Writing – review & editing, Validation, Software, Formal analysis. **Matthew McCoy:** Writing – review & editing, Writing – original draft, Validation, Software, Methodology, Formal analysis. **Michael J Pishvaian:** Writing – review & editing, Investigation. **Rosalie C Sears:** Writing – review & editing, Methodology, Investigation. **Jonathan R Brody:** Writing – review & editing, Resources, Methodology. **Charles J Yeo:** Writing – review & editing, Resources. **Aditi Jain:** Writing – review & editing, Writing – original draft, Visualization, Validation, Supervision, Software, Resources, Project administration, Methodology, Investigation, Funding acquisition, Formal analysis, Data curation, Conceptualization.

Declaration of competing interest

The authors declare that they have no known competing financial interests or personal relationships that could have appeared to influence the work reported in this paper.

Supplementary materials

Supplementary material associated with this article can be found, in the online version, at doi:10.1016/j.neo.2025.101152.

References

[1] C. de Juan, et al., Uncommon tumors and pseudotumoral lesions of the pancreas, Curr. Probl. Diagn. Radiol. 37 (4) (2008) 145–164.
[2] W. Park, A. Chawla, E.M. O'Reilly, Pancreatic Cancer: a review, JAMa 326 (9) (2021) 851–862.
[3] D.S. Dizon, A.H. Kamal, Cancer statistics 2024: all hands on deck, CA Cancer J. Clin. 74 (1) (2024) 8–9.
[4] V. Pandey, P. Storz, Targeting the tumor microenvironment in pancreatic ductal adenocarcinoma, Expert. Rev. AntiCancer Ther. 19 (6) (2019) 473–482.
[5] A. Jain, V. Bhardwaj, Therapeutic resistance in pancreatic ductal adenocarcinoma: current challenges and future opportunities, World J. Gastroenterol. 27 (39) (2021) 6527–6550.
[6] T. Conroy, et al., FOLFIRINOX or Gemcitabine as adjuvant therapy for pancreatic cancer, N. Engl. J. Med. 379 (25) (2018) 2395–2406.
[7] A. Chen, PARP inhibitors: its role in treatment of cancer, Chin. J. Cancer 30 (7) (2011) 463–471.
[8] N. Mekonnen, H. Yang, Y.K. Shin, Homologous recombination deficiency in ovarian, breast, colorectal, pancreatic, non-small cell lung and prostate cancers, and the mechanisms of resistance to PARP inhibitors, Front. Oncol. 12 (2022) 880643.
[9] S. Arora, et al., FDA approval summary: olaparib monotherapy or in combination with Bevacizumab for the maintenance treatment of patients with advanced ovarian cancer, Oncologist. 26 (1) (2021) e164–e172.
[10] T. Golan, et al., Maintenance Olaparib for Germline BRCA-mutated metastatic pancreatic cancer, N. Engl. J. Med. 381 (4) (2019) 317–327.
[11] H. Zhu, et al., PARP inhibitors in pancreatic cancer: molecular mechanisms and clinical applications, Mol. Cancer 19 (1) (2020) 49.
[12] M.J. Pishvaian, et al., A phase I/II study of Veliparib (ABT-888) in combination with 5-fluorouracil and oxaliplatin in patients with metastatic pancreatic cancer, Clin. Cancer Res. 26 (19) (2020) 5092–5101.
[13] W. Wong, et al., BRCA mutations in pancreas cancer: spectrum, current management, challenges and future prospects, Cancer Manage Res. 12 (2020) 2731–2742.
[14] F. Cimmino, D. Formicola, M. Capasso, Dualistic role of BARD1 in cancer, Genes. (Basel) 8 (12) (2017).
[15] R.M. Densham, et al., Human BRCA1-BARD1 ubiquitin ligase activity counteracts chromatin barriers to DNA resection, Nat. Struct. Mol. Biol. 23 (7) (2016) 647–655.
[16] W. Zhao, et al., BRCA1-BARD1 promotes RAD51-mediated homologous DNA pairing, Nature 550 (7676) (2017) 360–365.
[17] W. Zhao, et al., The BRCA tumor suppressor network in chromosome damage repair by homologous recombination, Annu. Rev. Biochem. 88 (2019) 221–245.
[18] M. Tarsounas, P. Sung, The antitumorigenic roles of BRCA1-BARD1 in DNA repair and replication, Nat. Rev. Mol. Cell Biol. 21 (5) (2020) 284–299.
[19] I. Irminger-Finger, W.C. Leung, BRCA1-dependent and independent functions of BARD1, Int. J. Biochem. Cell Biol. 34 (6) (2002) 582–587.
[20] I. Irminger-Finger, BARD1, a possible biomarker for breast and ovarian cancer, Gynecol. Oncol. 117 (2) (2010) 211–215.
[21] L. Li, et al., Oncogenic BARD1 isoforms expressed in gynecological cancers, Cancer Res. 67 (24) (2007) 11876–11885.
[22] Y. Liao, et al., Up-regulation of BRCA1-associated RING domain 1 promotes hepatocellular carcinoma progression by targeting Akt signaling, Sci. Rep. 7 (1) (2017) 7649.
[23] M. Pilyugin, et al., BARD1 serum autoantibodies for the detection of lung cancer, PLoS. One 12 (8) (2017) e0182356.
[24] L.I. McDougall, et al., Differential expression of BARD1 isoforms in melanoma, Genes. (Basel) 12 (2) (2021).
[25] A.K. Watters, et al., The effects of genetic and epigenetic alterations of BARD1 on the development of non-breast and non-gynecological cancers, Genes. (Basel) 11 (7) (2020).
[26] J.Y. Wu, et al., Aberrant expression of BARD1 in breast and ovarian cancers with poor prognosis, Int. J. Cancer 118 (5) (2006) 1215–1226.
[27] E. Dizin, I. Irminger-Finger, Negative feedback loop of BRCA1-BARD1 ubiquitin ligase on estrogen receptor alpha stability and activity antagonized by cancer-associated isoform of BARD1, Int. J. Biochem. Cell Biol. 42 (5) (2010) 693–700.
[28] Y.M. Hawsawi, et al., BARD1 mystery: tumor suppressors are cancer susceptibility genes, BMC. Cancer 22 (1) (2022) 599.
[29] O. Ozden, et al., Expression of an oncogenic BARD1 splice variant impairs homologous recombination and predicts response to PARP-1 inhibitor therapy in colon cancer, Sci. Rep. 6 (2016) 26273.
[30] Y. Zhu, et al., Tamoxifen-resistant breast cancer cells are resistant to DNA-damaging chemotherapy because of upregulated BARD1 and BRCA1, Nat. Commun. 9 (1) (2018) 1595.
[31] A. Jain, et al., HuR plays a role in double-strand break repair in pancreatic cancer cells and regulates functional BRCA1-associated-ring-domain-1(BARD1) isoforms, Cancers. (Basel) 14 (7) (2022).
[32] F. Cimmino, et al., Functional characterization of full-length BARD1 strengthens its role as a tumor suppressor in neuroblastoma, J. Cancer 11 (6) (2020) 1495–1504.
[33] M. Jimbo, et al., Targeting the mRNA-binding protein HuR impairs malignant characteristics of pancreatic ductal adenocarcinoma cells, Oncotarget. 6 (29) (2015) 27312–27331.
[34] T. Dhir, et al., Abemaciclib is effective against pancreatic cancer cells and synergizes with HuR and YAP1 inhibition, Mol. Cancer Res. 17 (10) (2019) 2029–2041.
[35] A. Jain, et al., Poly (ADP) ribose glycohydrolase can Be effectively targeted in pancreatic cancer, Cancer Res. 79 (17) (2019) 4491–4502.
[36] M. Hafner, et al., Growth rate inhibition metrics correct for confounders in measuring sensitivity to cancer drugs, Nat. Methods 13 (6) (2016) 521–527.
[37] A.O. Haber, et al., AraC-FdUMP[10](CF10) is a next generation fluoropyrimidine with potent antitumor activity in PDAC and synergy with PARG inhibition, Mol. Cancer Res. (2021).
[38] H. Hermeking, et al., Identification of CDK4 as a target of c-MYC, Proc. Natl. Acad. Sci. U S A 97 (5) (2000) 2229–2234.
[39] B.S. Nepon-Sixt, V.L. Bryant, M.G. Alexandrow, Myc-driven chromatin accessibility regulates Cdc45 assembly into CMG helicases, Commun. Biol. 2 (2019) 110.
[40] D.R. Reed, M.G. Alexandrow, Myc and the replicative CMG helicase: the creation and destruction of cancer: myc over-activation of CMG helicases drives tumorigenesis and creates a vulnerability in CMGs for therapeutic intervention, Bioessays 42 (4) (2020) e1900218.
[41] C. Wei, et al., Validating RRP12 expression and its prognostic significance in HCC based on data mining and bioinformatics methods, Front. Oncol. 12 (2022) 812009.
[42] A.S. Farrell, et al., MYC regulates ductal-neuroendocrine lineage plasticity in pancreatic ductal adenocarcinoma associated with poor outcome and chemoresistance, Nat. Commun. 8 (1) (2017) 1728.

[43] E. Kerkhoff, et al., Regulation of c-myc expression by Ras/Raf signalling, Oncogene 16 (2) (1998) 211–216.
[44] M.R. Silvis, et al., MYC-mediated resistance to trametinib and HCQ in PDAC is overcome by CDK4/6 and lysosomal inhibition, J. Exp. Med. 220 (3) (2023).
[45] M. Wirth, et al., Concepts to target MYC in pancreatic cancer, Mol. Cancer Ther. 15 (8) (2016) 1792–1798.
[46] J. Yao, et al., c-Myc-PD-L1 Axis sustained gemcitabine-resistance in pancreatic cancer, Front. Pharmacol. 13 (2022) 851512.
[47] S.H. Choi, et al., Myc protein is stabilized by suppression of a novel E3 ligase complex in cancer cells, Genes Dev. 24 (12) (2010) 1236–1241.
[48] I. Paul, et al., The ubiquitin ligase CHIP regulates c-myc stability and transcriptional activity, Oncogene 32 (10) (2013) 1284–1295.
[49] S.Y. Kim, et al., Skp2 regulates Myc protein stability and activity, Mol. Cell 11 (5) (2003) 1177–1188.
[50] M. Welcker, et al., A nucleolar isoform of the Fbw7 ubiquitin ligase regulates c-myc and cell size, Curr. Biol. 14 (20) (2004) 1852–1857.
[51] M. Welcker, et al., The Fbw7 tumor suppressor regulates glycogen synthase kinase 3 phosphorylation-dependent c-Myc protein degradation, Proc. Natl. Acad. Sci. U S A 101 (24) (2004) 9085–9090.
[52] T. Golan, et al., Strategies for the management of patients with pancreatic cancer with PARP inhibitors, Cancer Treat. Res. 186 (2023) 125–142.
[53] L. Oplustil O'Connor, et al., The PARP inhibitor AZD2461 provides insights into the role of PARP3 inhibition for both synthetic lethality and tolerability with chemotherapy in preclinical models, Cancer Res. 76 (20) (2016) 6084–6094.
[54] R. Huang, P.K. Zhou, DNA damage repair: historical perspectives, mechanistic pathways and clinical translation for targeted cancer therapy, Signal. Transduct. Target. Ther. 6 (1) (2021) 254.
[55] A. Tazzite, et al., BRCA mutational status is a promising predictive biomarker for platinum- based chemotherapy in triple-negative breast cancer, Curr. Drug Targets. 21 (10) (2020) 962–973.
[56] A. Klinakis, D. Karagiannis, T. Rampias, Targeting DNA repair in cancer: current state and novel approaches, Cell Mol. Life Sci. 77 (4) (2020) 677–703.
[57] E. Lai, et al., BRCA-mutant pancreatic ductal adenocarcinoma, Br. J. Cancer 125 (10) (2021) 1321–1332.
[58] T. Helleday, et al., DNA repair pathways as targets for cancer therapy, Nat. Rev. Cancer 8 (3) (2008) 193–204.
[59] C.G. Broustas, H.B. Lieberman, DNA damage response genes and the development of cancer metastasis, Radiat. Res. 181 (2) (2014) 111–130.
[60] Yin, M., F. Hong, and Q.E. Wang, *DNA damage response and cancer metastasis: clinical implications and therapeutic opportunities*, in *metastasis*, C.M. Sergi, editor. 2022: brisbane (AU).
[61] A.P. Wiegmans, et al., Rad51 supports triple negative breast cancer metastasis, Oncotarget. 5 (10) (2014) 3261–3272.
[62] E.L. Deer, et al., Phenotype and genotype of pancreatic cancer cell lines, Pancreas. 39 (4) (2010) 425–435.
[63] C. Xu, et al., The c-myc targeting hnRNPAB promotes lung adenocarcinoma cell proliferation via stabilization of CDK4 mRNA, Int. J. Biochem. Cell Biol. 156 (2023) 106372.
[64] E. Hessmann, et al., MYC in pancreatic cancer: novel mechanistic insights and their translation into therapeutic strategies, Oncogene 35 (13) (2016) 1609–1618.
[65] V. Bhardwaj, J. He, A. Jain, Glutamine stabilizes myc via alpha-ketoglutarate and regulates paclitaxel sensitivity, Med. Oncol. 39 (12) (2022) 227.
[66] R. Maddipati, et al., MYC levels regulate metastatic heterogeneity in pancreatic adenocarcinoma, Cancer Discov. 12 (2) (2022) 542–561.
[67] N.M. Sodir, et al., MYC instructs and maintains pancreatic adenocarcinoma phenotype, Cancer Discov. 10 (4) (2020) 588–607.
[68] E. Yeh, et al., A signalling pathway controlling c-myc degradation that impacts oncogenic transformation of human cells, Nat. Cell Biol. 6 (4) (2004) 308–318.
[69] N. Popov, et al., Fbw7 and Usp28 regulate myc protein stability in response to DNA damage, Cell Cycle 6 (19) (2007) 2327–2331.